Wrinkling in Sandwich Structures With a Functionally Graded Core

Victor Birman
Department of Mechanical and
Aerospace Engineering,
Missouri S&T Global—St. Louis,
Missouri University of Science and Technology,
12837 Flushing Meadows Drive,
St. Louis, MO 63131

Nam Vo
Department of Mechanical and
Aerospace Engineering,
Missouri University of Science and Technology,
Centennial Hall,
300 W 12th Street,
Rolla, MO 65409

This paper illustrates the effectiveness of a functionally graded core in preventing wrinkling in sandwich structures. The problem is solved for piecewise and continuous through-the-thickness core stiffness variations. The analysis is extended to account for the effect of temperature on wrinkling of a sandwich beam with a functionally graded core. The applicability of the developed theory is demonstrated for foam cores where the stiffness is an analytical function of the mass density. In this case, a desirable variation of the stiffness can be achieved by varying the mass density through the thickness of the core. Numerical examples demonstrate that wrinkling stability of a facing can significantly be increased using a piecewise graded core. The best results are achieved locating the layers with a higher mass density adjacent to the facing. A significant increase in the wrinkling stress can eliminate wrinkling as a possible mode of failure, without noticeably increasing the weight of the structure. In the case of a uniform temperature applied in addition to compression, wrinkling in a sandwich beam with a functionally graded core is affected both by its grading as well as by the effect of temperature on the facing and core properties. Although even a moderately elevated temperature may significantly lower the wrinkling stress, the advantage of a graded core over the homogeneous counterpart is conserved. [DOI: 10.1115/1.4034990]

Introduction

Sandwich structures consist of composite or isotropic facings supported by a foam, balsa, or honeycomb core. In addition to conventional cores, novel configurations, such as truss-reinforced cores have also been considered (e.g., Refs. [1,2]). The facings are thin, stiff, and relatively heavy, while the core is compliant and light. An analogy with an I-beam where the flanges may be likened to the facings and the web to the core is well known.

Reflecting on the complexity of sandwich structures, they possess a number of modes of failure. Possible failure modes include global modes, such as the loss of strength in the facings or core and the overall buckling of the structure and such local modes as wrinkling, core instability, and face dimpling over honeycomb cells. Fracture-related modes of failure, i.e., debonding of facings from core and delamination in composite facings should also be considered.

Wrinkling occurs when the facing develops local buckling waves under compression or in-plane shear. The length of the wrinkling wave is small compared to the planform dimensions of the sandwich panel, so that this local phenomenon is unaffected by the boundary conditions.

The wrinkling phenomenon is local, but it depends on the design of the sandwich panel joint and the relevant boundary conditions, as was demonstrated by Frostig [3]. In particular, if the compressive load is transferred to the panel through a rigid edge beam resulting in equal axial deformations of the facings and core, wrinkling occurs under controlled axial displacements, as is typical in experimental conditions or in a panel supported by stringers with a relatively large torsional stiffness maintaining uniform through the thickness axial deformations of the sandwich structure. However, if the compressive load is applied to the core, wrinkling is a result of controlled force loading. In the latter case, local three-dimensional effects near the edge are prominent and failure may occur due to the loss of strength prior to wrinkling. Furthermore, in the cases of an unsymmetrical panel or under bending where only one facing is undergoing compression, failure may occur by an overall buckling of the facing, rather than wrinkling.

There are numerous studies of wrinkling employing analytical and numerical methods. The pioneering research was published by Gough et al. [4], Hoff and Mautner [5], Plantema [6] and Allen [7]. These studies employed a variety of models, including the representation of the core as a continuous Winkler foundation, energy methods using the wrinkle-affected depth of the core and the length of the wrinkle as independent variables and the elasticity-based approach. Further analyses considering the problem of static and dynamic wrinkling under uniaxial and biaxial compression have been published by Vonach and Rammerstorfer [8–10], Gdoutos et al. [11], Kardomateas [12], Birman and Bert [13], Birman [14–16], Lim and Bart-Smith [17], and others. Early work on wrinkling in sandwich structures was reflected in review [18]. The papers by Sokolinsky and Frostig [19], Frostig et al. [3,20], Hohe et al. [20,21], and Phan et al. [22] are examples of work on static and dynamic wrinkling modeling the core by higher-order theories.

In the following analysis, we start with a reference to the studies where the stiffness of open-cell and closed-cell foams was expressed as a power function of their mass density. Accordingly, functional grading of foam cores can be prescribed in terms of the mass density varying through the thickness. The wrinkling problem in the case of a piecewise through-the-thickness grading is solved both using the equations of equilibrium and by an extension of the Hoff method. An extended Hoff method is also employed to solve the wrinkling problem for structure with a foam core with continuously varying mass density through the thickness. Numerical examples demonstrate that wrinkling stability of a facing can significantly be increased using a piecewise graded foam. The best results were achieved using denser and stiffer thin layers of foam adjacent to the facings and lighter foam in the interior of the core. In addition, we consider the effect of temperature on wrinkling in a sandwich beam with a functionally graded core. This analysis is limited to the range of temperature that does not trigger the onset of the conversion of polymeric materials in the facings and core into char. It is noted that even in the case of a homogeneous core, it may become effectively graded

Contributed by the Applied Mechanics Division of ASME for publication in the Journal of Applied Mechanics. Manuscript received July 7, 2016; final manuscript received October 10, 2016; published online November 7, 2016. Assoc. Editor: Dr. George Kardomateas.

due to a nonuniform through the thickness temperature and its effect on material constants. As is demonstrated in the example, the advantage of a sandwich structures with a functionally graded core is preserved at an elevated temperature.

Analysis

Consider a sandwich panel where one or both facings are subject to compression. An example of the facing supported by a functionally graded core consisting of several layers is shown in Fig. 1. The function of the grading is to increase the wrinkling stress by providing a stiffer support to the facing, while only marginally changing the weight of the structure. In particular, using functional grading is feasible in foam cores where the stiffness depends on their mass density [23]. The stiffness of polymeric foams may also be enhanced by selectively embedding stiff particles in the foam material achieving a desirable grading scheme [24].

The effective stiffness of foams was estimated in terms of their mass density by Gibson and Ashby [23,25]. The moduli of elasticity (E_c) and shear (G_c) of the foam were obtained in terms of the relative mass density with respect to that of the solid foam material and the stiffness of this material:

$$\frac{E_c}{E} = k_1 \left(\frac{\rho_c}{\rho}\right)^{n_1}, \quad \frac{G_c}{E} = k_2 \left(\frac{\rho_c}{\rho}\right)^{n_2} \tag{1}$$

where k_r and n_r $(r = 1, 2)$ are empirical constants, and E is the elastic modulus of the solid foam material. The Poisson ratio of foams was found nearly identical with that of the solid material.

Empirical constants for open-cell foams suggested in Ref. [25] were $k_1 = 1$, $k_2 = 0.4$, and $n_1 = n_2 = 2$. In experiments on closed-cell polyurethane foams Goods et al. [26] found $n_1 = 1.7$. Triantafillou and Gibson [27] experimented on closed-cell foams and estimated the values of the coefficients in the first Eq. (1) as $k_1 = 1.13$ and $n_1 = 1.71$.

An estimate of the stiffness of a closed-cell foam was suggested in Ref. [23] distinguishing between the fraction of the foam material contained in the cell struts φ and the fraction of the material contained in the walls $(1 - \varphi)$

$$\begin{aligned} \frac{E_c}{E} &= \varphi^2 \left(\frac{\rho_c}{\rho}\right)^2 + (1-\varphi)\left(\frac{\rho_c}{\rho}\right) \\ \frac{G_c}{E} &= \frac{3}{8}\left[\varphi^2 \left(\frac{\rho_c}{\rho}\right)^2 + (1-\varphi)\left(\frac{\rho_c}{\rho}\right)\right] \end{aligned} \tag{2}$$

Theory of Elasticity Approach to the Analysis of Wrinkling in the Case of a Piecewise Functionally Graded Core. Consider a foam core including thin layers of a constant mass density (and constant stiffness) adjacent to the facing, Fig. 1. The analysis

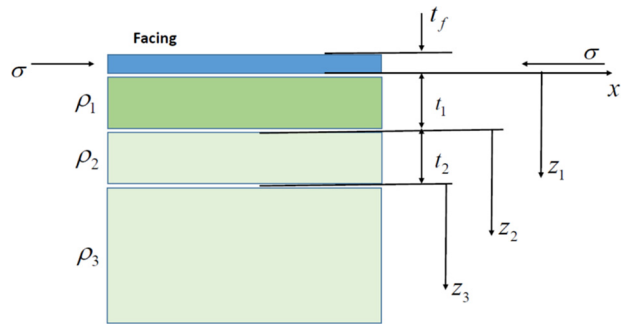

Fig. 1 The facing of a sandwich structure supported by a functionally graded core. The wrinkling stress is increased by using stiffer outer layers: $\rho_1 > \rho_2 > \rho_3$.

extends the solution in paper [14] where the core stresses were estimated using the theory of elasticity solution. This approach enables us to exactly satisfy the stress equilibrium equation in the thickness direction, while the equilibrium equation in the axial direction is satisfied in the integral sense. This is an improvement over the classical Hoff method where all equations of equilibrium are violated.

The elasticity solution for sandwich panels and beams with a homogeneous core was developed by Kardomateas [12]. This is a very accurate solution, accounting for finite rigidity of the core in both axial and thickness directions. Considering a homogeneous core, the solution utilizes the buckling differential equations in terms of displacements. Such equations are not valid if the stiffness of the core is a continuous function of the coordinates. In case where the stiffness tensor of the core is a stepwise function of coordinates, the solution in Ref. [12] can be adopted though it would require a consideration of the buckling equations for each homogeneous layer of the core and subsequently finding the wrinkling stress through a satisfaction of the continuity conditions along the interfaces of the layers. Such analysis is outside the scope of the present paper.

Consider wrinkling of a sandwich panel or beam where the section of the core adjacent to the facing consists of several layers. The facing wrinkling deformation is assumed in the form

$$w = W \sin \frac{\pi x}{l} \tag{3}$$

where W and l are the amplitude and length of the wrinkle, and x is the coordinate collinear with the applied load (Fig. 1).

The equations of the theory of elasticity in the i-th homogeneous layer of the core are

$$\begin{aligned} \sigma_x^{(i)}{}_{,x} + \tau_{xz}^{(i)}{}_{,z} &= 0 \\ \tau_{xz}^{(i)}{}_{,x} + \sigma_z^{(i)}{}_{,z} &= 0 \end{aligned} \tag{4}$$

where all notations are standard.

The constitutive relations for an isotropic layer of the foam core are

$$\begin{aligned} \sigma_x^{(i)} &= Q_{11}^{(i)}\varepsilon_x + Q_{13}^{(i)}\varepsilon_z \\ \sigma_z^{(i)} &= Q_{13}^{(i)}\varepsilon_x + Q_{11}^{(i)}\varepsilon_z \\ \tau_{xz}^{(i)} &= G^{(i)}\gamma_{xz} \end{aligned} \tag{5}$$

As is typical in the wrinkling analysis, the plane strain condition implies that $\varepsilon_y = 0$.

The linear strain–displacement relationships are

$$\begin{aligned} \varepsilon_x^{(i)} &= u^{(i)}{}_{,x} \\ \varepsilon_z^{(i)} &= w^{(i)}{}_{,z} \\ \gamma_{xz}^{(i)} &= u^{(i)}{}_{,z} + w^{(i)}{}_{,x} \end{aligned} \tag{6}$$

where u and w are the axial and transverse displacements, respectively.

The axial displacements in the core under the wrinkle are neglected in such models as those of Hoff and Mautner [5] and Plantema [6]. Physically, this superimposes an additional constraint on the structure, increasing the predicted wrinkling stress. While Hoff attributed a difference between his theory and experimental data to initial imperfections in the facings, the effect of such artificial constraint may be another source of such discrepancy. It should be noted that wrinkling waves usually appear in patterns including several parallel waves. The adjacent wrinkles of the facing are antisymmetric relative to the point of their junction, so that if they were considered without a reference to deformations of the entire panel, the axial displacement of the junction point would be zero. This implies that deformation waves in the

core under adjacent wrinkles constrain each other's axial displacements, somewhat justifying the assumption that these displacements are negligible. Assuming that axial displacements in the core are negligible, and simplifying the strain–displacement relations accordingly, we obtain upon the substitution of Eqs. (5) and (6) into Eq. (4) the following equations of equilibrium

$$\begin{aligned} w^{(i)}{}_{,xz} &= 0 \\ Q_{11}^{(i)} w^{(i)}{}_{,zz} + G^{(i)} w^{(i)}{}_{,xx} &= 0 \end{aligned} \tag{7}$$

The solution within each homogeneous layer of the core is sought in the form

$$w^{(i)} = X^{(i)}(x) Z^{(i)}(z_i) \tag{8}$$

where z_i is the thickness coordinate of the i-th layer as shown in Fig. 1.

The substitution of Eq. (8) into the second equation of equilibrium (7) and the separation of variables yield

$$Q_{11}^{(i)} \frac{Z_i(z_i)_{,z_i z_i}}{Z_i(z_i)} = -G^{(i)} \frac{X_i(x)_{,xx}}{X_i(x)} = C^{(i)} \tag{9}$$

where $C^{(i)}$ is a constant that is different for each layer.

The solution of Eq. (9) is

$$\begin{aligned} X_i(x) &= C_3^{(i)} \sin f_i \lambda_i x + C_4^{(i)} \cos f_i \lambda_i x \\ Z_i(z_i) &= C_3^{(i)} \sin\, h\lambda_i z_i + C_2^{(i)} \cos\, h\lambda_i z_i \end{aligned} \tag{10}$$

In these equations, $C_j^{(i)}$ $(j = 1, 2, 3, 4)$ are constants of integration and

$$\lambda_i = \sqrt{\frac{C^{(i)}}{Q_{11}^{(i)}}}, \quad f_i = \sqrt{\frac{Q_{11}^{(i)}}{G^{(i)}}} \tag{11}$$

The sinusoidal shape of deformation in the core is assumed unchanged from layer to layer implying that $C_4^{(i)} = 0$ and

$$f_i \lambda_i = \frac{\pi}{l} \tag{12}$$

As follows from this equation, constants

$$C^{(i)} = \left(\frac{\pi}{l}\right)^2 G_c^{(i)} \tag{13}$$

Furthermore, without the loss of accuracy, we can set $C_3^{(i)} = W$.

Although the first equilibrium Eq. (7) cannot be exactly satisfied, it is satisfied in the integer sense, i.e., $\int_0^l w_{,xz} dx = 0$. This inaccuracy is the consequence of neglecting the axial displacement adopted in the Hoff method and in the present analysis.

The mode of wrinkling was discussed by Hoff and other researchers (e.g., see Ref. [5]) considering symmetric and antisymmetric patterns of wrinkles in both facings with respect to the middle plane. The antisymmetric mode of wrinkles is rather typical for sandwich panels, as is reflected in the results in Ref. [12]. Note that in case of wrinkling of the compressed facing in a panel subject to bending, the opposite facing is subject to tension, and it does not wrinkle. This case can also be analyzed using the present solution.

In the first case considered here, wrinkling occurs simultaneously in both equally compressed facings, and the wrinkling waves are symmetric or antisymmetric about the middle plane of the core. The entire core is affected and accounting for symmetry about the middle plane, and constants of integration are determined from the condition of continuity of the displacements at the facing–core interface and the conditions of continuity of displacements and normal and transverse shear strains at the interface between the adjacent core layers. In the case of symmetric wrinkling, the additional symmetry condition is that the displacement at the middle plane of the sandwich is equal to zero. Accordingly, in the case of symmetric wrinkling

$$\begin{aligned} &Z_1(z_1 = 0) = 1 \\ &Z_1(z_1 = t_1) = Z_2(z_2 = 0) \\ &Z_1'(z_1 = t_1) = Z_2'(z_2 = 0) \\ &\cdots\cdots\cdots\cdots\cdots\cdots\cdots\cdots\cdots\cdots \\ &Z_i(z_i = t_i) = Z_{i+1}(z_{i+1} = 0) \\ &Z_i'(z_i = t_i) = Z_{i+1}'(z_{i+1} = 0) \\ &\cdots\cdots\cdots\cdots\cdots\cdots\cdots\cdots\cdots\cdots \\ &Z_N\left(z_N = \frac{t_N}{2}\right) = 0 \end{aligned} \tag{14}$$

where t_i is the thickness of the i-th layer of the core, $(\ldots)' = (d(\ldots)/dz)$, $1 < i < N$, and N is the number of layers from one of the facings to the middle plane, including the N-th layer that is bisected by this plane. It is observed that the number of unknown constants of integration $C_1^{(i)}$, $C_2^{(i)}$ equals the number of equations (14).

If wrinkling is antisymmetric, the continuity conditions (14) are enforced throughout the entire depth of the core, but the last Eq. (14) is replaced with

$$Z_{2N}(z_{2N} = t_{2N}) = 1 \tag{15a}$$

where $2N$ is the total number of core layers between two facings.

In the other case considered here only one facing wrinkles. This occurs if the opposite facing is stiffer or it is not subject to compression. In such case, Eq. (14) remains valid, except for the last equation that is replaced with

$$Z_{2N}(z_{2N} = t_{2N}) = 0 \tag{15b}$$

In all cases the constants of integration determined from the systems of algebraic equations (14) (and Eq. (15*a*) or Eq. (15*b*), if applicable) are used to calculate λ_i from Eq. (11). Subsequently, the stresses in the layers of the core are obtained using Eqs. (5), (6), (8), and (10). These stresses are employed in the extended Hoff formulation discussed below. Contrary to the classical Hoff method, the solution presented in this section does not rely on the assumption that the depth of the core affected by the wrinkle is limited. Accordingly, the only independent variable affecting the wrinkling stress is the length of the wrinkle l.

It should be noted that the choice of an extension of Hoff's method in the subsequent analysis is justified by recent experimental findings [1], where this method was found in better agreement with test data on panels with a homogeneous core than several alternative methods.

The total potential energy per unit width of the panel is composed of the strain energies of the facing and core, and the energy of the applied load that is the opposite of work of this force. The expressions for the energy of the facing and the energy of the applied compressive load reproduced from the Hoff solution are unaffected by the structure of the core. The former energy is

$$U_f = \frac{D_f}{2} \int_0^l (w_{,xx})^2 dx = \frac{\pi^4 D_f}{4l^3} W^2 \tag{16}$$

where D_f is the bending stiffness of the facing.

The work of the wrinkling stresses σ_{wr} applied to the facing is

$$V_{\text{wr}} = \frac{\sigma_{\text{wr}} t_f}{2} \int_0^l (w_{,x})^2 dx = \frac{\pi^2 t_f W^2}{4l} \sigma_{\text{wr}} \tag{17}$$

where t_f is the thickness of the facing.

The energy of the core includes the contributions of all layers. For example, in the first case considered above, i.e., if both facings wrinkle symmetrically

$$U_c = \frac{1}{2}\int_0^l \sum_{i=1}^{N} \int_{z_i=0}^{z_i=t_i} \frac{\left(\sigma_z^{(i)}\right)^2}{Q_{11}{}^{(i)}} dxdz + \frac{1}{2}\int_0^l \sum_{i=1}^{N} \int_{z_i=0}^{z_i=t_i} \frac{\left(\tau_{xz}^{(i)}\right)^2}{G^{(i)}} dxdz \tag{18}$$

The axial stress in the core does not directly contribute to the strain energy since $\sigma_x^{(i)} = 0$, according to the assumption adopted above.

The substitution of the expressions for the layerwise stresses and integration of Eq. (18) over the axial coordinate yield

$$U_c = \frac{l}{4}W^2 \sum_{i=1}^{N} \left\{ Q_{11}^{(i)} \int_{z_i=0}^{z_i=t_i} \left[Z_i(z_i)_{,z}\right]^2 dz + \left(\frac{\pi}{l}\right)^2 G^{(i)} \int_{z_i=0}^{z_i=t_i} \left[Z_i(z_i)\right]^2 dz \right\} \tag{19}$$

The wrinkling stress can now be determined as a function of the only independent variable, i.e., the length of the wrinkle

$$\begin{aligned} \sigma_{\text{wr}} &= \min\left\{ \frac{1}{\pi^2 t_f}\left(\frac{\pi^4 D_f}{l^2} + l^2 F\right) \right\} \\ F &= \sum_{i=1}^{N} \left\{ Q_{11}^{(i)} \int_{z_i=0}^{z_i=t_i} \left[Z_i(z_i)_{,z}\right]^2 dz + \left(\frac{\pi}{l}\right)^2 G^{(i)} \int_{z_i=0}^{z_i=t_i} \left[Z_i(z_i)\right]^2 dz \right\} \\ &= f_1 + \left(\frac{\pi}{l}\right)^2 f_2 \\ f_1 &= \sum_{i=1}^{N} Q_{11}^{(i)} \int_{z_i=0}^{z_i=t_i} \left[Z_i(z_i)_{,z}\right]^2 dz, \quad f_2 = \sum_{i=1}^{N} G^{(i)} \int_{z_i=0}^{z_i=t_i} \left[Z_i(z_i)\right]^2 dz \end{aligned} \tag{20}$$

The minimization is conducted resulting in both the length of the wrinkle and the wrinkling stress

$$l_{\text{wr}} = \pi \sqrt[4]{\frac{D_f}{f_1}}, \quad \sigma_{\text{wr}} = \frac{1}{t_f}\left(2\sqrt{D_f f_1} + f_2\right) \tag{21}$$

The case where only one facing wrinkles is analyzed similarly.

The number of wrinkling waves at the critical load can be determined using the length of the wrinkle given by Eq. (21). In theory, the wrinkles appear over the entire surface of the panel, so given its length, the number of identical wrinkles is available. In reality, boundary conditions may affect the wrinkles adjacent to the edge (see, for example, local three-dimensional effects in the vicinity to the edge subject to controlled force demonstrated in Ref. [3]). Furthermore, even small local defects may affect wrinkling, triggering only one or several waves, prior to wrinkling of the entire panel.

Analysis of Wrinkling of a Sandwich Panel or Beam With a Continuously Functionally Graded Core Using the Hoff Method. The Hoff method (sometimes called the Hoff–Mautner method) utilizes the assumption that displacements in the core in the direction perpendicular to the facing decrease linearly with the distance from the facing–core interface [5]

$$w = W\frac{h-z}{h}\sin\frac{\pi x}{l} \tag{22}$$

where h is the depth of the core affected by wrinkling.

We apply this method to the case where the core of the sandwich structure is continuously graded through the thickness. Then, the equations of equilibrium have variable coefficients and cannot exactly be integrated.

The difference between the Hoff method applied to a sandwich structure with a homogeneous core as compared to the counterpart with a functionally graded core appears in the expression for the strain energy of the core. While the strain energy of the facing and the work of the applied load are given by Eqs. (16) and (17), the strain energy of the core in a sandwich beam is

$$U_c = \frac{1}{2}\int_0^l \int_0^h \frac{\sigma_z^2}{E(z)} dxdz + \frac{1}{2}\int_0^l \int_0^h \frac{\tau_{xz}^2}{G(z)} dxdz \tag{23}$$

where the stresses are given by

$$\sigma_z = E(z)w_{,z}, \quad \tau_{xz} = G(z)w_{,x} \tag{24}$$

In the case of a sandwich panel, the same approach is used replacing the modulus of elasticity $E(z)$ with reduced stiffness $Q_{11}(z)$.

Substituting the expressions for graded moduli of elasticity and shear as well as the wrinkling mode shape given by Eq. (22) in the integrals in Eq. (23), the strain energy of the core becomes

$$U_c = \left[\left(\frac{\pi}{l}\right)^2 F_1(h) + F_2(h)\right]\frac{l}{4}W^2 \tag{25}$$

where

$$F_1(h) = \int_0^h G(z)\left(\frac{h-z}{h}\right)^2 dz, \quad F_2(h) = \frac{1}{h^2}\int_0^h E(z)dz \tag{26}$$

Combining Eqs. (16), (17), and (25) to obtain the total potential energy, the wrinkling stress is explicitly derived as

$$\sigma_{\text{wr}} = \frac{1}{\pi^2 t_f}\left\{\frac{\pi^4 E_f}{l^2} + l^2\left[\left(\frac{\pi}{l}\right)^2 F_1(h) + F_2(h)\right]\right\} \tag{27}$$

where E_f is a bending modulus of the facing replacing the bending stiffness D_f in Eq. (16).

The minimization of the wrinkling stress with respect to the wrinkle depth and length depends on the functional grading of the core, i.e., $E(z)$ and $G(z)$. Once these functions are specified and the integrals in Eq. (26) are evaluated, the solution is straightforward. The solution for the wrinkling stress of a sandwich structure with a homogeneous core considered as a particular case of the above solution coincides with the classical Hoff formula.

Wrinkling Stress in a Sandwich Beam Exposed to an Elevated Temperature. The effect of an elevated temperature on structures involves both explicit "thermal" terms in the expressions for the strains, stresses, stress resultants, and stress couples as well as the effect of temperature on the material properties. In polymeric composites, the latter effect if further complicated by a decomposition of the material, viscous softening, oxidation, etc. (e.g., see Ref. [28]). A comprehensive thermomechanical analysis requires the solution of coupled problems of heat transfer, decomposition and property degradation, and thermomechanical static or dynamic formulation. In the case involving functionally graded materials, the solution becomes even more complicated due to a different effect of temperature at various locations in the graded medium. All material constants, such as specific heat capacity, thermal conductivity, and thermal expansion coefficients and the stiffness tensor, vary both with the location as well as with the local temperature.

The effect of fire is an example of a rigorous thermomechanical analysis in sandwich structures [29–33]. In the case of polymeric composite facings and a polymeric or balsa core, the properties of the material as well as the stiffness of the structure exposed to fire

continuously change with time as the polymer or balsa is converted into char. The charred regions gradually expand through the thickness of the structure until it collapses.

In the wrinkling problem considered here, we assume a quasi-static uniform or nonuniform through the thickness temperature distribution. The analysis is limited to the case where the elevated temperature is not sufficient to trigger the char conversion process (e.g., for a vinylester resin the char onset temperature is between 250 °C and 300 °C [34]). The heat conduction problem is assumed solved. Accordingly, given the local temperature, the property degradation can be determined by one of available curve–fitting relationships [28].

Polynomial Relationship

$$P(T) = \left[1 - \sum_{j=1} k_j \left(\frac{T - T_0}{T_g - T_0}\right)^j\right] P_0 \tag{28}$$

where P is the property in question, T is a current temperature, T_g is the glass transition temperature, T_0 and P_0 are a reference temperature and the corresponding property at this temperature, k_j are empirical coefficients and is a natural number.

An alternative model is represented by the so-called "tan h equation"

$$P(T) = \left\{\frac{P_0 + P_R}{2} - \frac{P_0 - P_R}{2} \tan h\left[k(T - T_g)\right]\right\} \tag{29}$$

where P_R is a fully relaxed (high temperature) property of the composite. The property–temperature relationships accounting for additional phenomena taking place under an elevated temperature are discussed elsewhere (e.g., see Ref. [30]).

In fiber-reinforced facings relationships (28) and (29) may be available for the composite material or for the individual phases (e.g., a polymer matrix may be affected by an elevated temperature that has a negligible effect on the fiber material). In the latter case, Eqs. (28) or (29) should be employed to account for the degradation of the corresponding constituent phases in an appropriate micromechanical formulation yielding the property of the composite material of the facing.

In the foam core, the properties of the solid foam material should be adjusted at an elevated temperature. For example, using the property degradation Eq. (28), the modulus of elasticity of a solid foam material in Eqs. (1) and (2) is

$$E(T) = \left[1 - \sum_{j=1} k_j \left(\frac{T - T_0}{T_g - T_0}\right)^j\right] E(T_0) \tag{30}$$

An alternative simple relationship approximately estimating the stiffness of the foam as a linear function of temperature is [23]

$$E(T) = \left(1 - \alpha_m \frac{T}{T_g}\right) E(T_{K=0}) \tag{31}$$

where $E(T_{K=0})$ is the modulus of elasticity at $T = 0°\text{K}$, and α_m is a constant that varies in the range $\alpha_m = 0.5 \pm 0.2$. For rigid polyurethane foams, the appropriate constant value is $\alpha_m = 0.65$.

Experimental data for such foam materials as polyurethanes (e.g., see Ref. [35]) generally supports a nearly linear relationship between the stiffness and temperature above 0 °C, with some nonlinearity that could be accommodated using Eq. (30). Data for rigid polyurethane foams presented in Ref. [23] demonstrated that the stiffness of the foam changes linearly with temperature in accordance with Eq. (31), in the range of relative foam densities varying from 0.06 to 0.35 and for temperatures increasing up to 200 °C.

In the case of a sandwich beam affected by a uniform temperature, the thermally induced property degradation is monitored by the relationships presented above. The subsequent analysis is conducted generalizing the previous solutions to account for explicit thermal terms. For example, the strains for the i-th isotropic layer are obtained by a generalization of Eq. (6)

$$\begin{aligned} \varepsilon_x &\equiv \varepsilon_x^{(i)} = u^{(i)}{}_{,x} - \alpha^{(i)} T \\ \varepsilon_z &\equiv \varepsilon_z^{(i)} = w^{(i)}{}_{,z} - \alpha^{(i)} T \\ \gamma_{xz} &\equiv \gamma_{xz}^{(i)} = u^{(i)}{}_{,z} + w^{(i)}{}_{,x} \end{aligned} \tag{32}$$

where $\alpha^{(i)} = \alpha^{(i)}(T)$ is the coefficient of thermal expansion. Following the Hoff method, the strain–displacement relations can be simplified in the subsequent analysis by neglecting the axial displacement.

Using the shape of the wrinkle (3), the solution of the equations of equilibrium (4) remains without change, i.e., it is given by Eq. (8), but the continuity conditions (14) and (15) are modified. For example, for a symmetric sandwich beam experiencing symmetric wrinkling, Eqs. (14) are replaced with

$$\begin{aligned} &Z_1(z_1 = 0) = 1 \\ &Z_1(z_1 = t_1) = Z_2(z_2 = 0) \\ &Z_1{}'(z_1 = t_1) - \alpha^{(1)} T = Z_2{}'(z_2 = 0) - \alpha^{(2)} T \\ &\cdots\cdots\cdots\cdots\cdots\cdots\cdots\cdots\cdots\cdots \\ &Z_i(z_i = t_i) = Z_{i+1}(z_{i+1} = 0) \\ &Z_i{}'(z_i = t_i) - \alpha^{(i)} T = Z_{i+1}{}'(z_{i+1} = 0) - \alpha^{(i+1)} T \\ &\cdots\cdots\cdots\cdots\cdots\cdots\cdots\cdots\cdots\cdots \\ &Z_N\left(z_N = \frac{t_N}{2}\right) = 0 \end{aligned} \tag{33}$$

In the case of a uniform temperature, Eq. (33) guarantee the continuity of both the displacements as well as the axial (ε_z) and transverse shear strains (γ_{xz}) at the interfaces between the adjacent core layers.

It is noted that even if the core is homogeneous, it becomes effectively graded when the structure is exposed to a nonuniform through the thickness temperature. This grading is due to the effect of such temperature on the core properties. Contrary to the intentional grading of the core that benefits wrinkling stability, a temperature-induced grading is usually undesirable. For example, if the structure is subject to a heat flux (fire) at one surface, temperature in the core adjacent to the exposed surface is higher, and the stiffness is lower than in a more remote from this surface section of the core.

Numerical Examples

The numerical analysis was undertaken for three different facings, i.e., glass/epoxy, E-glass/vinyl ester, and graphite epoxy AS 3501 cross-ply facings. The properties of these materials are [36]

$$\begin{aligned} &\text{Glass/epoxy}: E_1 = 38.6\,\text{GPa}, \quad E_2 = 8.27\,\text{GPa}, \quad G_{12} = 4.14\,\text{GPa}, \\ &\nu_{12} = 0.26, \; V_f = 0.45 \end{aligned}$$

$$\begin{aligned} &E - \text{glass/vinylester}: E_1 = 24.4\,\text{GPa}, \; E_2 = 6.87\,\text{GPa}, \\ &G_{12} = 2.89\,\text{GPa}, \quad \nu_{12} = 0.32, \quad V_f = 0.30 \end{aligned}$$

$$\begin{aligned} &AS3501\,\text{graphite/epoxy}: E_1 = 138.0\,\text{GPa}, \; E_2 = 9.0\,\text{GPa}, \\ &G_{12} = 6.9\,\text{GPa}, \; \nu_{12} = 0.30, \; V_f = 0.65 \end{aligned}$$

where V_f is the volume fraction of fibers.

The thickness of the facing was equal to 2 mm, each layer being 0.25 mm thick. In panels with such thin facings, wrinkling may

occur at a lower stress than the loss of strength. The alternative failure mode, i.e., global buckling, that is not considered here depends on the thickness and the span of the sandwich beam. The core material was polyurethane foam with the mass density ratio varying from 10% to 35% of the solid polyurethane. The properties of solid polyurethane are $\rho = 1200\,\mathrm{kg/m^3}$, $E = 1.6\,\mathrm{GPa}$ [23].

The core adjacent to the facing was subdivided into three sections (Fig. 1). The mass densities of foam in the outer sections 1 and 2 were larger than that in the inner section 3, $\rho_1 \geq \rho_2 \geq \rho_3$. The wrinkling stress was normalized with respect to its counterpart in the structure with a homogeneous core of the mass density equal to 10% of that of the solid polyurethane, $\rho_3 = 0.10\rho$. The core was assumed thick, so that the opposite facing did not affect the analysis.

The effect of the thickness of functionally graded sections of the core on the wrinkling stress is demonstrated in Fig. 2. Even very thin denser layers supporting the facing may result in a large increase in the wrinkling stress (over 50%, even if layers 1 and 2 are only 2 mm thick). This illustrates the potential of functional grading that can be achieved with a negligible increase in the weight of the structure.

The effect of using a thicker intermediate layer (layer 2) is illustrated in Fig. 3. The beneficial effect of a higher mass density (and stiffness) of the intermediate layer is limited. Predictably, a more pronounced effect on wrinkling stability is achieved by increasing the thickness of the outermost layer adjacent to the facing (layer 1), as demonstrated in Fig. 4.

The effect of varying the mass density of layer 2 is further demonstrated in Figs. 5 and 6 for two different thickness values $t_1 = t_2$. A useful observation from these figures is that even using a single denser layer adjacent to the facing (layer 2 eliminated, so that $(\rho_2/\rho) - 0.1$) can result in a significant increase in the wrinkling stress (over 50% improvement with $t_1 = t_2 = t_f$ and over 170% with $t_1 = t_2 = 4t_f$ for graphite epoxy facings and even better results for glass/epoxy and E-glass/vinyl ester facings). The effect of an increase of the mass density of the outermost layer (layer 1) is depicted in Figs. 7 and 8, where the wrinkling stress sharply increases as the mass density of the outermost layer increases from that for layer 2 $\rho_1 = \rho_2 = 0.20\rho$ to the maximum value considered in these examples, i.e., $\rho_1 = 0.35\rho$.

The envelopes of the required mass densities of layers 1 and 2 necessary to increase the wrinkling stress by factor of 2.0 as compared to the wrinkling stress for a beam with a homogeneous foam core of the mass density equal to 0.10ρ, are shown in Fig. 9. As is reflected in the previous discussion and evidenced from the figure, a desirable wrinkling stability improvement can be achieved with a denser outermost layer, while increasing the mass density of the intermediate layer is less efficient.

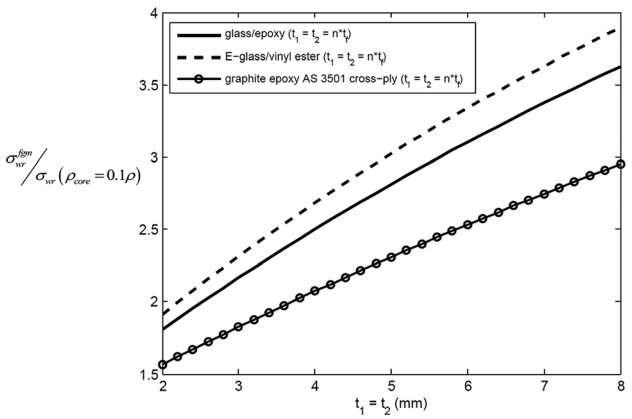

Fig. 2 Effect of variations in the thickness of a functionally graded core on the wrinkling stress. The mass density of the core layers are $\rho_1 = 0.35\rho$, $\rho_2 = 0.15\rho$, and $\rho_3 = 0.10\rho$, the thicknesses of layers 1 and 2 are equal to each other.

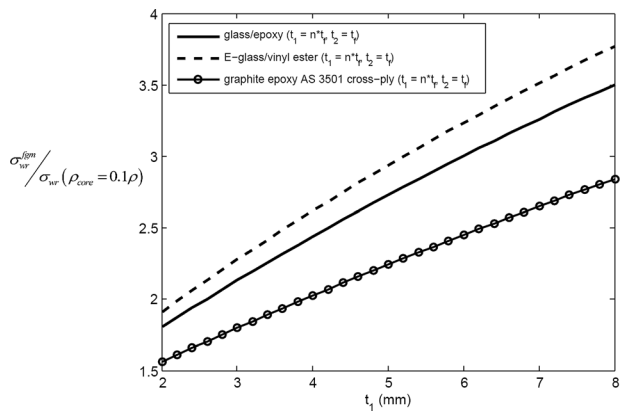

Fig. 4 Effect of variations in the thickness of outermost layer 1 in a functionally graded core on the wrinkling stress. The thickness of intermediate layer 2 is $t_2 = t_f$. The mass density of the core layers are $\rho_1 = 0.35\rho$, $\rho_2 = 0.15\rho$, and $\rho_3 = 0.10\rho$. The thickness of layer 1 varies from t_f (2 mm) to $4t_f$ (8 mm).

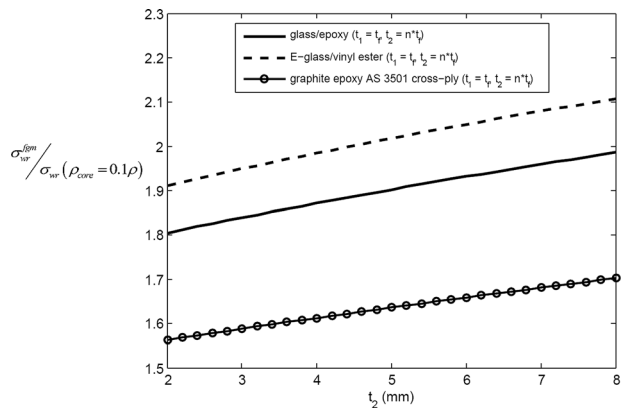

Fig. 3 Effect of variations in the thickness of intermediate layer 2 in a functionally graded core on the wrinkling stress. The thickness of outermost layer 1 is $t_1 = t_f$. The mass density of the core layers are $\rho_1 = 0.35\rho$, $\rho_2 = 0.15\rho$, and $\rho_3 = 0.10\rho$. The thickness of layer 2 varies from t_f (2 mm) to $4t_f$ (8 mm).

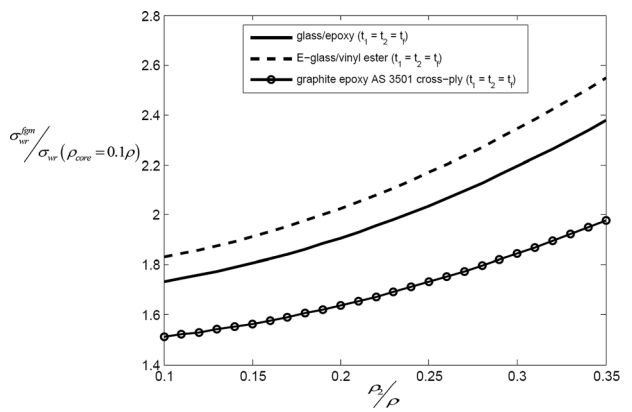

Fig. 5 Effect of variations in the mass density of intermediate layer 2 in a functionally graded core on the wrinkling stress. The mass density of the core layers are $\rho_1 = 0.35\rho$, $\rho_3 \leq \rho_2 \leq \rho_1$, and $\rho_3 = 0.10\rho$, the thicknesses of layers 1 and 2 are equal to $t_1 = t_2 = t_f$.

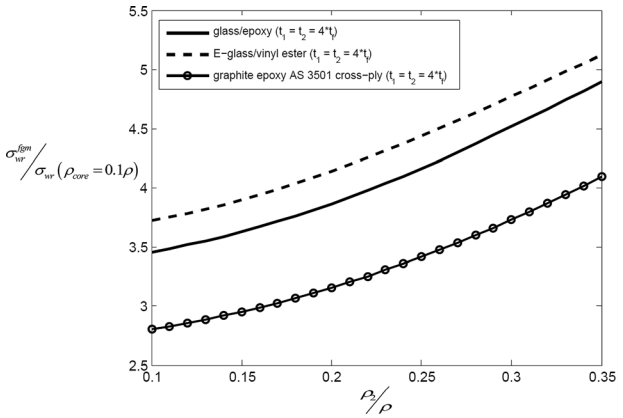

Fig. 6 Effect of variations in the mass density of intermediate layer 2 in a functionally graded core on the wrinkling stress. The mass density of the core layers are $\rho_1 = 0.35\rho$, $\rho_3 \le \rho_2 \le \rho_1$, and $\rho_3 = 0.10\rho$, the thicknesses of layers 1 and 2 are equal to $t_1 = t_2 = 4t_f$.

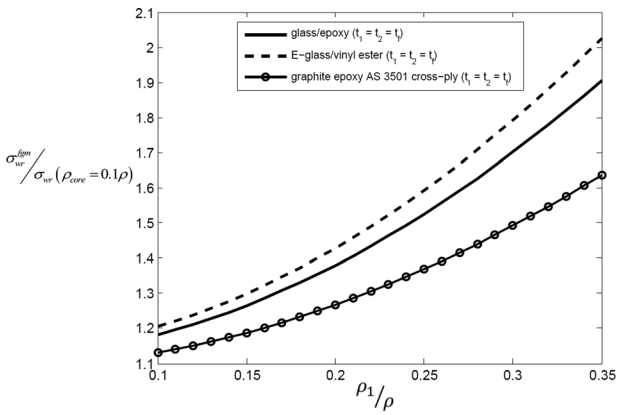

Fig. 7 Effect of variations in the mass density of outermost layer 1 in a functionally graded core on the wrinkling stress. The mass density of the core layers are $\rho_2 \le \rho_1 \le 0.35\rho$, $\rho_2 = 0.20\rho$, and $\rho_3 = 0.10\rho$, the thicknesses of layers 1 and 2 are equal to $t_1 = t_2 = t_f$.

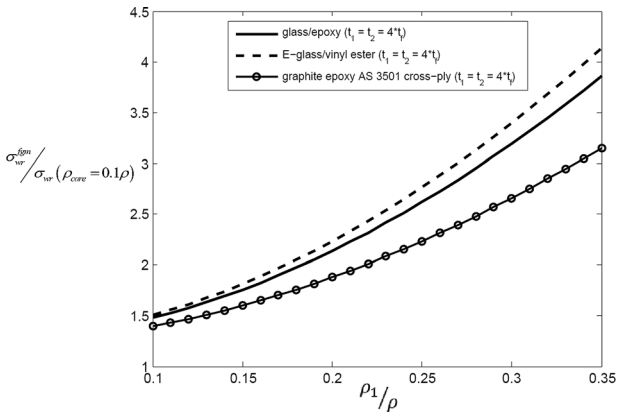

Fig. 8 Effect of variations in the mass density of outermost layer 1 in a functionally graded core on the wrinkling stress. The mass density of the core layers are $\rho_2 \le \rho_1 \le 0.35\rho$, $\rho_2 = 0.20\rho$, and $\rho_3 = 0.10\rho$, the thicknesses of layers 1 and 2 are equal to $t_1 = t_2 = 4t_f$.

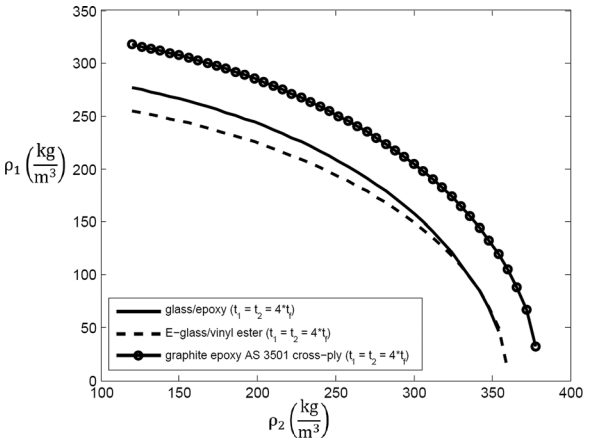

Fig. 9 Failure envelopes for mass densities of layers 1 and 2 necessary to increase the wrinkling stress by a factor of 2.0 compared to a homogeneous core of mass density $\rho_3 = 0.1\rho = 120\ kg/m^3$. The thicknesses of layers 1 and 2 are equal to $t_1 = t_2 = 4t_f$.

The effect of an increase of the uniform temperature from 0 °C to 100 °C on the wrinkling stress is demonstrated on the example of a sandwich beam with quasi-isotropic E-glass vinyl ester facings and a polyurethane foam core. The core was constructed of three layers, the outermost layer with the mass density $(\rho_c/\rho) = 0.35$, the intermediate layer $(\rho_c/\rho) = 0.19$, and the inner layer $(\rho_c/\rho) = 0.13$. The thicknesses of the facings and two outer layers were equal to $t_f = t_1 = t_2 = 2$ mm. The half-thickness of the inner layer (the distance from the interface with layer 2 and the middle plane) was $t_3 = 6$ mm. The stiffness of the solid polyurethane foam material adopted in this example was reported in Refs. [23,37]. The experimentally measured moduli of elasticity of the foam at the reference temperature 0 °C were equal to

$$E_c = 0.45\,\text{GPa}\,((\rho_c/\rho) = 0.35),\ E_c = 0.15\,\text{GPa}\,((\rho_c/\rho) = 0.19),\ \text{and}$$
$$E_c = 0.08\,\text{GPa}\,((\rho_c/\rho) = 0.13)$$

At 100 °C, the corresponding stiffness values were

$$E_c = 0.25\,\text{GPa}\,((\rho_c/\rho) = 0.35),\ E_c = 0.10\,\text{GPa}\,((\rho_c/\rho) = 0.19)\ \text{and}$$
$$E_c = 0.05\,\text{GPa}\,((\rho_c/\rho) = 0.13)$$

The values reported in Refs. [23,37] were found in a good agreement with the predicted stiffness according to Eq. (31). The shear moduli of the core layers were estimated using the Poisson ratio equal to 0.375 that was unaffected by mass density or temperature.

The stiffness of quasi-isotropic facings was adopted from Ref. [38] being equal to 20.5 GPa at 0 °C and 17.9 GPa at 100 °C. These values are somewhat higher than those reported for cross-ply E-glass vinyl ester laminates in Ref. [39] but the general trend was unchanged. The stiffness and strength of E-glass vinyl ester abruptly decrease at temperatures slightly higher than 100 °C, i.e., this temperature is close to the maximum service temperature for this material.

The wrinkling stress at 100 °C was equal to only 63% of the counterpart at 0 °C (0.43 GPa and 0.68 GPa, respectively). However, even at this elevated temperature, the wrinkling stress of the sandwich beam with a functionally graded core was higher than that of the homogeneous beam with $(\rho_c/\rho) = 0.13$ by a factor of 2 demonstrating that the advantage of a functionally graded core is preserved at elevated temperatures.

Conclusions

This paper presents the analysis of wrinkling in sandwich structures with functionally graded cores. Two grading models are considered, i.e., a continuously varying stiffness of the core and the core consisting of several layers, each layer having a different stiffness. For the latter case, the benefits of using a graded core in preventing wrinkling instability have been demonstrated. It is shown that a desirable increase of the wrinkling stress can be achieved using thin layers of a stiffer core adjacent to the facing. Increasing the thickness of the stiffer section of the core adjacent to the facing results in a large increase in the wrinkling stress. A similar outcome is achieved increasing the stiffness of the core adjacent to the facing.

In the presence of an elevated temperature, the degradation of both typical core materials as well as polymeric composite facings results in a smaller wrinkling stress, even if the transformation into char does not occur. However, if the temperature is uniform through the thickness, the advantages of using a functionally graded core in preventing wrinkling are preserved.

It should be noted that while the wrinkling stress can be increased using a functionally graded core, the effect of such modification on the overall buckling of the structure remains minimal since the stiffness of the core remains much lower than that of the facings. An increase of the wrinkling stress is beneficial only if wrinkling is the mode of failure of the sandwich structure. For example, the wrinkling stress should not be increased beyond the value corresponding to failure in the layers of the facing. Wrinkling may become the dominant mode of failure if the facings are thin, and the core is too compliant to provide sufficient support.

References

[1] Tuwair, H., Volz, J., ElGawady, M. A., Chandrashekhara, K., and Birman, V., 2016, "Modeling and Analysis of GFRP Bridge Deck Panels Filled With Polyurethane Foam," J. Bridge Eng., **21**(5), p. 04016012.

[2] Tuwair, H., Volz, J., Elgawady, M. A., Mohamed, M., Chandrashekhara, K., and Birman, V., 2016, "Testing and Evaluation of Polyurethane-Based GFRP Sandwich Bridge Deck Panels With Polyurethane Foam Core," J. Bridge Eng., **21**(1), p. 04015033.

[3] Frostig, Y., 2011, "On Wrinkling of a Sandwich Panel With a Compliant Core and Self-Equilibrated Loads," J. Sandwich Struct. Mater., **13**(6), pp. 663–679.

[4] Gough, G. S., Elam, C. F., and deBruyne, N. A., 1940, "The Stabilization of a Thin Sheet by a Continuous Support Medium," J. R. Aeronaut. Soc., **44**(349), pp. 12–43.

[5] Hoff, N. J., and Mautner, S. E., 1945, "The Buckling of Sandwich-Type Panels," J. Aeronaut. Sci., **12**(3), pp. 285–297.

[6] Plantema, F. J., 1966, *Sandwich Construction*, Pergamon Press, New York.

[7] Allen, H. G., 1969, *Analysis and Design of Structural Sandwich Panels*, Pergamon Press, Oxford.

[8] Vonach, W. K., and Rammerstorfer, F. G., 2001, "A General Approach to the Wrinkling Instability of Sandwich Plates," Struct. Eng. Mech., **12**(4), pp. 363–376.

[9] Vonach, W. K., and Rammerstorfer, F. G., 2000, "Wrinkling of Thick Orthotropic Sandwich Plates Under General Loading Conditions," Arch. Appl. Mech., **70**(5), pp. 338–348.

[10] Vonach, W. K., and Rammerstorfer, F. G., 2000, "Effects of In-Plane Core Stiffness on the Wrinkling Behavior of Thick Sandwiches," Acta Mech., **141**(1), pp. 1–10.

[11] Gdoutos, E. E., Daniel, I. M., and Wang, K. A., 2003, "Compression Facing Wrinkling of Composite Sandwich Structures," Mech. Mater., **35**(3–6), pp. 511–522.

[12] Kardomateas, G. A., 2005, "Wrinkling of Wide Sandwich Panels/Beams With Orthotropic Phases by an Elasticity Approach," ASME J. Appl. Mech., **72**(6), pp. 818–825.

[13] Birman, V., and Bert, C. W., 2004, "Wrinkling of Composite-Facing Sandwich Panels Under Biaxial Loading," J. Sandwich Struct. Mater., **6**(3), pp. 217–237.

[14] Birman, V., 2004, "Thermomechanical Wrinkling in Composite Sandwich Structures," AIAA J., **42**(7), pp. 1474–1479.

[15] Birman, V., 2005, "Thermally Induced Bending and Wrinkling in Large Aspect Ratio Sandwich Panels," Compos. Part A: Appl. Sci. Manuf., **36**(10), pp. 1412–1420.

[16] Birman, V., 2004, "Dynamic Wrinkling in Sandwich Beams," Compos. Part B: Eng., **35**(6–8), pp. 665–672.

[17] Lim, J. Y., and Bart-Smith, H., 2015, "An Analytical Model for the Face Wrinkling Failure Prediction of Metallic Corrugated Core Sandwich Columns in Dynamic Compression," Int. J. Mech. Sci., **92**, pp. 290–303.

[18] Noor, A. K., Burton, W. S., and Bert, C. W., 1996, "Computational Models for Sandwich Panels and Shells," ASME Appl. Mech. Rev., **49**(3), pp. 155–199.

[19] Sokolinsky, V., and Frostig, Y., 2000, "Branching Behavior in the Nonlinear Response of Sandwich Panels With a Transversely Flexible Core," Int. J. Solids Struct., **37**(40), pp. 5745–5772.

[20] Hohe, J., Librescu, L., and Oh, S. Y., 2006, "Dynamic Buckling of Flat and Curved Sandwich Panels With Transversely Compressible Core," Compos. Struct., **74**(1), pp. 10–24.

[21] Hohe, J., and Librescu, L., 2008, "Recent Results on the Effect of the Transverse Core Compressibility on the Static and Dynamic Response of Sandwich Structures," Compos. Part B: Eng., **39**(1), pp. 108–119.

[22] Phan, C. N., Bailey, N. W., Kardomateas, G. A., and Battley, M. A., 2012, "Wrinkling of Sandwich Wide Panels/Beams Based on the Extended High-Order Sandwich Panel Theory: Formulation, Comparison With Elasticity and Experiments," Arch. Appl. Mech., **82**(10–11), pp. 1585–1599.

[23] Gibson, L. J., and Ashby, M. F., 1997, *Cellular Solids, Structure and Properties*, Cambridge University Press, Cambridge, UK.

[24] Birman, V., Chandrashekhara, K., Hopkins, M. S., and Volz, J. S., 2013, "Effects of Nanoparticle Impregnation of Polyurethane Foam Core on the Performance of Sandwich Beams," Compos. Part B: Eng., **46**, pp. 234–246.

[25] Gibson, L. J., and Ashby, M. F., 1982, "Mechanics of Three-Dimensional Cellular Materials," Proc. R. Soc. London, Ser. A, **382**(1782), pp. 43–59.

[26] Goods, S. H., Neuschwanger, C. L., Whinnery, L. L., and Nix, W. D., 1999, "Mechanical Properties of a Particle-Strengthened Polyurethane Foam," J. Appl. Polym. Sci., **74**(11), pp. 2724–2736.

[27] Triantafillou, T. C., and Gibson, L. J., 1987, "Failure Mode Maps for Foam Core Sandwich Beams," Mater. Sci. Eng., **95**(C), pp. 37–53.

[28] Mouritz, A. P., Feih, S., Kandare, E., Mathys, Z., Gibson, A. G., Des Jardin, P. E., Case, S. W., and Lattimer, B. Y., 2009, "Review of Fire Structural Modelling of Polymer Composites," Compos. Part A: Appl. Sci. Manuf., **40**(12), pp. 1800–1814.

[29] Liu, L., Holmes, J. W., Kardomateas, G. A., and Birman, V., 2011, "Compressive Response of Composites Under Combined Fire and Compression Loading," Fire Technol., **47**(4), pp. 985–1016.

[30] Gibson, A. G., Wu, Y. S., Evans, J. T., and Mouritz, A. P., 2006, "Laminate Theory Analysis of Composites Under Load in Fire," J. Compos. Mater., **40**(7), pp. 639–658.

[31] Feih, S., Mathys, Z., Gibson, A. G., and Mouritz, A. P., 2007, "Modelling the Tension and Compression Strengths of Polymer Laminates in Fire," Compos. Sci. Technol., **67**(3–4), pp. 551–564.

[32] Birman, V., Kardomateas, G. A., Simitses, G. J., and Li, R., 2006, "Response of a Sandwich Panel Subject to Fire or Elevated Temperature on One of the surfaces," Compos. Part A: Appl. Sci. Manuf., **37**(7), pp. 981–988.

[33] Kardomateas, G. A., Simitses, G. J., and Birman, V., 2009, "Structural Integrity of Composite Columns Subject to Fire," J. Compos. Mater., **43**(9), pp. 1015–1033.

[34] Anjang, A., Chevali, V. S., Lattimer, B. Y., Case, S. W., Feih, S., and Mouritz, A. P., 2015, "Post-Fire Mechanical Properties of Sandwich Composite Structures," Compos. Struct., **132**, pp. 1019–1028.

[35] Chiou, B., and Schoen, P. E., 2002, "Effects of Crosslinking on Thermal and Mechanical Properties of Polyurethanes," J. Appl. Polym. Sci., **83**(1), pp. 212–223.

[36] Gibson, R. F., 2007, *Principles of Composite Material Mechanics*, CRC Press, Boca Raton.

[37] Traeger, R. K., 1967, "Physical Properties of Rigid Polyurethane Foams," J. Cell. Plast., **3**(9), pp. 405–418.

[38] Kulkarni, A., and Gibson, R., 2003, "Nondestructive Characterization of Effects of Temperature and Moisture on Elastic Moduli of Vinyl Ester Resin and E-Glass/Vinylester Composite," American Society of Composites 18th Annual Technical Conference, Paper No. 122.

[39] Gibson, A. G., Browne, T., Feih, S., and Mouritz, A. P., 2012, "Modeling Composite High Temperature Behavior and Fire Response Under Load," J. Compos. Mater., **46**(16), pp. 2005–2022.